Boiling Heat Transfer in Battery Electric vehicles

EEVC
Brussels, Belgium, October 26-28, 2011

Boiling Heat Transfer in Battery Electric Vehicles

Rob van Gils[1,*], Michel Speetjens[2], Henk Nijmeijer[1]
[1]*Eindhoven University of Technology, Department of Mechanical Engineering, Dynamics and Control group*
[2]*Eindhoven University of Technology, Department of Mechanical Engineering, Energy Technology group*
[*]*Corresponding author, P.O Box 513, WH -1.144, 5600 MB, Eindhoven,* r.w.v.gils@tue.nl

Abstract

In this paper the feedback stabilisation of a boiling-based cooling scheme is discussed. Application of such cooling schemes in practical setups is greatly limited by the formation of a thermally insulating vapour film on the to-be-cooled device, called burn-out. In this study a first step is made, to check the viability of such cooling systems, already used in high performance electronics, applied to Electric Vehicles (EVs). It can be used for instance for the cooling of high heat flux transistors and for the thermal homogenisation of battery packs. Thereto, the unstable transition to burn-out is stabilised by controlling the pressure inside the boiling chamber, with which boiling (and thus creation of the thermally insulating vapour film) can be stimulated or suppressed. The feedback law used to do this is based on the dominant modes of the temperature field of the thermally conducting element, i.e. the heater, between the device and the boiling liquid. As not all states used in this feedback law can be measured, an observer or "state-estimator" must be implemented in the control strategy. The observer is a copy of the nonlinear boiling model with an additional term to assure convergence of observer to system state. Simulations are performed to demonstrate controller efficiency on the nonlinear cooling device. This puts forth the boiling-based cooling scheme as viable for application in EVs, enabling increased cooling and thermal-homogenisation capacities compared to conventional thermal management methods. The next step should be experiments to proof the principle on battery cells/packs and high heat flux transistors.

Keywords: BEV, Battery thermal management, Cooling, boiling, numerical simulation

1 Introduction

During fast acceleration and regenerative braking in electric vehicles (EVs), the high-power switching devices, that switch large amounts of power from the battery pack to the electrical coils of the electric motors, produce significant amounts of heat. To prevent these so-called insulated gate bipolar transistors (IGBTs) from overheating during these actions, boiling heat transfer is the pre-eminent choice as the cooling mechanism. Boiling heat transfer namely allows for *quick* and *intensive* cooling. Moreover, the evaporated fluid can be easily transported throughout the vehicle, and the removed heat can be released to any desired surface via condensation. In this way, the removed heat can be used, for instance to heat the vehicle cabin, decreasing the auxiliary power requirements. In addition, due to natural convection, no (large) pumps are required to circulate the fluids. Thus thermal management based on boiling heat transfer can significantly increase the range per charge of Battery Electric Vehicles (BEVs) [1], which is currently considered to be their main drawback, [2].
Boiling heat transfer can also be applied as battery thermal management system. Operation at elevated temperatures can seriously accelerate battery deterioration, see [3]. While operation at lowered temperatures can seriously decrease the efficiency of the battery, see [1]. Furthermore, due to the passive working principle, boiling heat transfer can also be applied when the car is turned off, e.g. when the car is parked in the sun. Another important parameter with respect

to the battery lifespan is the temperature uniformity of the battery, see [4]. Hence, especially in consideration of cycle life of the battery pack, a thermal management/homogenisation scheme is indispensable. Boiling heat transfer allows for thermal homogenisation very effectively as it, irrespective of heat fluxes, happens at fixed temperatures for given pressure, see [5].
However, full exploitation of boiling heat transfer for thermal management is severely limited by the risk of 'burn-out', i.e. the sudden formation of a vapour blanket on the heating device that leads to a catastrophic temperature jump and, in consequence, an abrupt collapse of the cooling and homogenisation capacity [6]. Insight into the complex boiling dynamics underlying "burn-out" and into ways to actively control it, is imperative to overcome this hazard.
Pool boiling may serve as physical representation for cooling applications based on boiling heat transfer. Such systems consist of a heater submerged in a pool of boiling liquid. This is depicted in Fig.1, the to-be-cooled device supplies heat to the bottom wall of the heater, which corresponds with a thermally conducting element between the actual heat source (e.g. a battery cell) and the coolant at the top wall of the heater. The boiling liquid extracts heat from the heater and releases thermal energy through the escaping vapour. The vapour turns into liquid again in a condenser, releasing the heat taken up, and flows back towards the boiling liquid.

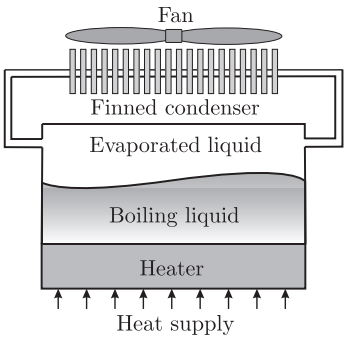

Figure 1: Schematic representation of a pool-boiling system.

Pool boiling is characterised by three boiling regimes through which the system progresses with increasing temperature on the fluid-heater interface: nucleate, transition and film boiling [7]. Nucleate boiling is, as opposed to film boiling, an efficient and safe mode of heat transfer and is the desired boiling mode in most practical applications. Nucleate boiling transits into film boiling upon exceeding the so-called critical heat flux (CHF) through the intermediate state of transition boiling. This transition is highly unstable and causes a sharp *increase* in temperature and *decrease* in heat flux. This is the result of the sudden formation of a thermally-insulating vapour film on the fluid-heater interface [6]. Transition, thus, leads to the collapse of the cooling and homogenisation capacity and must be avoided in practical thermal management systems [7].

Hence, utilising boiling heat transfer for cooling entails a trade-off between efficiency (close proximity to CHF) and safe operation (certain distance from CHF). Current cooling schemes require a relatively large safety margin due to two key limitations: (i) high uncertainty in predicting CHF and system dynamics; (ii) the inability to actively respond to fluctuating cooling demands due to the passive working principle [8]. Robust control strategies that safely facilitate boiling heat transfer close to CHF under dynamic operating conditions offer a promising solution, yet their realisation poses a formidable challenge.

As a result, to date theoretical studies for pool boiling applications are scarce. There is a large data-base on boiling experiments, though. However, the CHF depends, next to the fluid-heater combination, on numerous other variables, such as surface roughness and system pressure. Consequently, experimental results can only be used in a very limited range of boiling applications, see e.g. [6, 9]. Theoretical pool boiling investigations are presented in [10] where a one-dimensional (1D) system is stabilised by way of linearisation of the boiling curve around the homogeneous transition state. In [11] a more realistic pool boiling model is formulated which leans on the phenomenological connection between the local boiling mode and the interface temperature and describes the system dynamics entirely in terms of the temperature distribution within the heater. In [12, 13] the two-dimensional (2D) nonlinear heater-only model is analysed for equilibria and stability properties. Successful stabilisation of the one-dimensional (1D) simplification of this model has been achieved in [14] by regulation of the heat supply via a linear state feedback based on the internal temperature profile. Most recent investigations of stabilisation of unstable steady states of the original 2D model are presented in [15, 16].

Key to the proposed control strategy is the expression of the heater's temperature profile by Chebyshev and Fourier polynomials, which are intimately related to the physical eigenmodes of the 2D system. The smoothness of the temperature field within the heater ensures exponential convergence of the Chebyshev-Fourier spectrum and, consequently, accurate representation of its eigenmodes by lower-order Chebyshev and Fourier polynomials. This has the important implication that the system dynamics can be regulated on the basis of a few lower-order Fourier-Chebyshev modes of the temperature field.

This study aims to test this 2D modal control law for the purpose of thermal management in EVs by way of a performance analysis in an idealised system as first step towards realisation of a practical setup. Thereto, the dynamical behaviour of the system introduced in [16] is considered for realistic values of the physical parameters. The control law represents the dynamical variation of the system pressure, with which the onset of film boiling is to be prevented. The simulations represent two thermal issues in EVs, being (i) IGBT-cooling and (ii) thermal homogenisation of the battery pack. These simulations are a first step towards realisation of a practical setup.

For the IGBT-cooling case study, a 80×80mm IGBT that produces 15W/cm^2 of heat is considered [17]. For the second case study the thermal homogenisation of a small battery cell, like for example used in the Tesla Roadster, 65mm of length, is considered. The cell is assumed to produce 0.33W/cm^2 of heat [18]. In both cases the heater is assumed to be made out of aluminum with dimensions $L \times H$. Its length is equal to that of the to-be-conditioned device: $L = 80$mm for the IGBT and $L = 65$mm for the battery cell. Its height is to be specified hereafter. The fluorinated liquid FC-72 (C_6F_{14}, 3M company) with a boiling point of $T_{\text{sat}} = 56°$C at atmospheric pressure, is considered to be the coolant.

2 Model description

The model to represent the thermal management scheme is based upon the two-dimensional (2D) heater-only model first presented in [12]. In this model, the boiling fluid is solely modelled by the boundary condition on top of the heater. This can be done because of a phenomenological connection between the boiling mode and the interface temperature, cf. [12]. In the following, this model, its equilibria and the linearisation around them are discussed.

2.1 Heater-only model

In the heater-only model, the heat transfer in the 2D rectangular heater $\mathcal{H} = [0, L] \times [0, H]$ is considered – see Fig.2. The boundary segments of the heater are given by (i) adiabatic sidewalls for $x = 0$ and $x = L$, (ii) a constant heat supply extended with the system input by which unstable states must be stabilised at $y = 0$, and (iii) the nonlinear heat extraction by the boiling process on top of the heater at $y = H$.

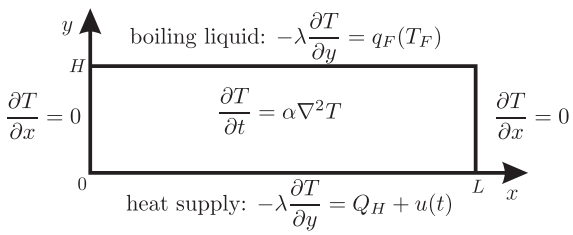

Figure 2: Heater configuration of the pool-boiling model.

The model describes the heat transfer in terms of the superheat $T(x, y, t)$, i.e. the temperature relative to the boiling point of the coolant. The superheat $T(x, y, t)$ within the heater is given by the heat equation

$$\frac{\partial T}{\partial t}(x, y, t) = \alpha\nabla^2 T(x, y, t), \tag{1}$$

with the boundary conditions

$$\left.\frac{\partial T}{\partial x}\right|_{x=0,L} = 0, \tag{2}$$

$$\left.\frac{\partial T}{\partial y}\right|_{y=0} = -\frac{1}{\lambda}(Q_H + u(t)), \tag{3}$$

$$\left.\frac{\partial T}{\partial y}\right|_{y=H} = -\frac{1}{\lambda}q_F(T_F), \tag{4}$$

with $\lambda = 237$Wm^{-1}K^{-1} the thermal conductivity of the aluminum heater, L its length as defined in the Introduction, H its height, $T_F := T(x, H, t)$ the fluid-heater interface temperature, $\alpha = 8.42 \cdot 10^{-5}$m^2/s the thermal diffusivity of the heater, $q_F(T_F)$ the nonlinear heat flux relation given in Fig.3, $u(t)$ the system input and Q_H the nominal heat generation by the to-be-cooled device as defined in the introduction.
Burn-out is to be avoided by variation of the system pressure. Decreasing (increasing) p stimulates (suppresses) evaporation and thus will lead to burn-out faster (less fast). Decreasing (increasing) the pressure will thus decrease (increase) the CHF, i.e. the local maximum of $q_F(T_F)$ in Fig. 3, CHF $\propto p$. Although reduction (elevation) of the pressure is accompanied by a temperature decrease (increase), the temperature distribution will remain uniform and heat flux per unit area will remain high. By regulating the pressure, the system thus can be kept in the efficient nucleate boiling regime. In the model, decreasing (increasing) the system pressure is modelled by increasing (decreasing) the heat supply $Q_H + u(t)$, which will lead to burn-out faster (less fast), $u(t) \propto \text{CHF}^{-1} \propto p^{-1}$. As a result, the heat flux function $q_F(T_F)$ can be kept constant over time and system modelling simple.

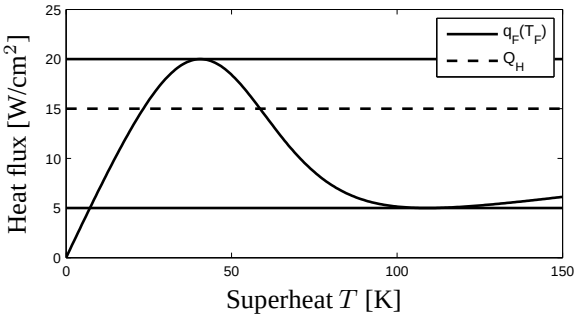

Figure 3: Nonlinear heat-flux function $q_F(T_F)$ according to the boiling curve of aluminum vs. FC-72, see [9]. The dashed line represents the nominal heat supply Q_H.

The nonlinear heat-flux function $q_F(T_F)$ describes the *local* heat exchange between the heater and the boiling fluid as function of the *local* fluid-heater interface temperature. On physical grounds, it is identified with the so-called

boiling curve, that is, the relation describing the *mean* heat exchange between heater and fluid along the *entire* fluid-heater interface (see [7]). This implies a functional relation $q_F(T_F)$ according to Fig.3. As can be seen, the function q_F comprises three distinct regimes, these correspond to one of the local boiling modes and associated boiling states: nucleate boiling (left of local maximum; fluid-rich state, efficient heat transfer), transition boiling (in between both extremes; transitional state) and film boiling (right of local minimum; vapour-rich state, inefficient heat transfer). If the heat supply exceeds CHF, the nucleate boiling regime ceases to exist, and passing through the transition boiling regime, the film boiling regime is entered. This is accompanied with a massive increase in temperature and thus is to be avoided in practical applications.

2.2 Equilibria of the model

An extensive exposition on the steady states of this model and their stability properties is furnished in [12, 13]. Below a concise recapitulation is provided.
Steady states $T_\infty(x, y)$ of (1-4) are found via application of the method of separation of variables, see [19]. This yields a (formal) solution given by

$$T_\infty(x,y) = \sum_{k=0}^{\infty} \widetilde{T}_k \frac{\cosh(\kappa_k y)}{\cosh(\kappa_k H)} \cos(\kappa_k x) + \frac{Q_H}{\lambda}(H-y), \tag{5}$$

with $\kappa_k = k\pi/L$ and coefficients $\widetilde{T}_k$ the spectrum of the Fourier cosine expansion of the temperature at the fluid-heater interface,

$$T_{F,\infty}(x) := T_\infty(x,H) = \sum_{k=0}^{\infty} \widetilde{T}_k \cos(\kappa_k x). \tag{6}$$

These coefficients are determined by the nonlinear Neumann condition at $y = H$, upon substitution of (5) leading to

$$\sum_{k=0}^{\infty} \widetilde{T}_k \kappa_k \tanh(\kappa_k H)\cos(\kappa_k x) - \frac{Q_H}{\lambda} = -\frac{1}{\lambda} q_F(T_{F,\infty}), \forall\ x \in [0,L]. \tag{7}$$

Equation (7) is the characteristic equation that determines the particular properties of the steady states of (1-4). If $\widetilde{T}_k = 0$ for $k > 0$, the equilibrium is constant in x-direction and (7) simplifies to $q_F(T_{F,\infty}) = Q_H$. As a result, $T_{F,\infty}$ coincides with the intersection(s) between the boiling curve (solid line in Fig.3) and the nominal heat-supply (dashed line in Fig.3). Here the left and right intersections correspond to stable nucleate and stable film boiling, respectively. The middle intersection corresponds to an unstable transition boiling equilibrium. These three equilibria are called the homogeneous equilibria as they are uniform in x-direction. All other equilibria are not uniform in x-direction and are called the heterogeneous equilibria. Heterogeneous solutions are characterised by local liquid-rich and local vapour-rich regions and thus belong to the transition boiling regime.
The principal objective here is the stabilisation of the unstable homogeneous transition equilibrium. Without stabilisation of this equilibrium, exceeding the CHF will inherently result in progression to the film boiling regime and burn-out of the to-be-cooled device. Stabilisation of this equilibrium, on the other hand, allows for increased heat flux rates and thus increases the efficiency of the cooling device. Because of the non-uniform temperature distribution of the heterogeneous equilibria, convergence towards these equilibria results in undesired non-uniform temperature distributions in the battery pack or IGBT and thus is to be avoided during operation.

2.3 Linearisation

Stabilisation of the homogeneous transition boiling equilibrium is investigated in terms of a linearisation of the pool boiling model around this equilibrium. To this end, small deviations $v(x, y, t)$ from the equilibrium $T_\infty(x, y)$ are considered, i.e. $T(x, y, t) = T_\infty(x, y) + v(x, y, t)$. Standard linearisation methods readily yield

$$\frac{\partial v}{\partial t}(x,y,t) = \alpha \nabla^2 v(x,y,t), \tag{8}$$

with the boundary conditions

$$\left.\frac{\partial v}{\partial x}\right|_{x=0,L} = 0, \tag{9}$$

$$\left.\frac{\partial v}{\partial y}\right|_{y=0} = -\frac{1}{\lambda}u(t), \tag{10}$$

$$\left.\frac{\partial v}{\partial y}\right|_{y=H} = -\frac{1}{\lambda}\gamma(x) v_F(x), \tag{11}$$

as linear counterpart of (1-4), where $v_F(x) := v(x, H)$ and

$$\gamma(x) = \left.\frac{\mathrm{d}q_F}{\mathrm{d}T_F}\right|_{T_F(x)=T_{F,\infty}(x)}. \tag{12}$$

3 Control strategy

In this section, the control strategy for stabilisation of the pool boiling system is discussed. Burn-out is to be avoided by variation of the system pressure p. In order to keep the heat flux function $q_F(T_F)$ constant over time and system modelling simple, this is modelled by uniform variation $u(t)$ of the heat supply, as discussed in the previous section.

3.1 Feedback law

The intended control strategy is a feedback law based on the deviation $v(x,y,t) = T(x,y,t) - T_\infty(x,y)$ between the heater superheat $T(x,y,t)$ and its desired distribution $T_\infty(x,y)$. Easily stated, if the temperature inside the heater is lower than the desired value, $u(t)$ is positive as a result of which boiling is stimulated and lower heat fluxes are generated between heater and boiling liquid. Consequently, the device is cooled less efficient and heats itself. When the temperature is too high, the input is negative and boiling is suppressed by increasing the pressure, as a result, higher heat fluxes are generated and more heat is extracted from the device, cooling it down in the process.
The input can be calculated by evaluating the heaters temperature in only one or two specific points, however, the aim here is to evaluate the entire temperature profile in the feedback law in favor of beneficial closed-loop behaviour, i.e. the behaviour of the system with the feedback law. The heater temperature $v(x,y,t)$ is multiplied with a feedback weightfunction $g(x,y)$ to be able to give more weight to specific regions within the heater, e.g. the fluid-heater interface. As system pressure is equal in the entire boiling chamber, the system input $u(t)$ must be uniform in x-direction. As a result, the term $v(x,y,t)g(x,y)$ must be integrated over the heater domain, resulting in the feedback law

$$u(t) = \int_0^H \int_0^L v(x,y,t)g(x,y)\mathrm{d}x\mathrm{d}y. \quad (13)$$

This means that the controller calculates whether the overall temperature in the heater is too high or too low and stimulates or suppresses the boiling process accordingly (specific regions can be excluded or be given more weight by appropriate choice of $g(x,y)$). With the feedback weight function the properties of the feedback law, and thus the closed-loop system, will be prescribed. Furthermore, the temperature inside the heater $v(x,y,t)$ is expressed in a form that is intimately related to its natural eigenmodes. This means that in x-direction, the eigenmodes of the Laplace operator are taken to represent the profile, i.e. by a Fourier-cosine expansion. In y-direction, the profile is expressed in the non-periodic variant of this expansion, i.e. the Chebyshev expansion. This control law is discussed in full detail in [15, 16], here only a concise recapitulation is given. The temperature profile in terms of the Chebyshev-Fourier spectrum is given by

$$v(x,y,t) = \sum_{k,n=0}^{\infty} \widetilde{v}_{nk}(t)\phi_n(\theta(y))\rho_k(x), \quad (14)$$

with $\widetilde{v}_{nk}$ the spectral coefficients of $v(x,y,t)$, $\phi_n(\theta) = \cos(n\arccos(\theta))$ is the n-th Chebyshev polynomial, $\rho_k(x) = \cos(\kappa_k x)$ the k-th Fourier cosine polynomial and $\theta = \frac{2}{H}y - 1$ is the computational domain in y-direction, cf. [20]. Note that here an infinite series is considered, meaning no approximation error is introduced in this step. Moreover, if a smooth temperature field in the heater is assumed, due to exponential convergence of the Chebyshev-Fourier-cosine spectral coefficients, the system dynamics are mainly prescribed by the 'lower order' modes, i.e. modes with low n *and* low k. As a result, the feedback law given by (13) only needs to be based on these 'lower' modes, as established in [14].
In order to filter these specific modes from the profile $v(x,y,t)$, the feedback weight function $g(x,y)$ is taken as

$$g(x,y) = \sum_{q,p=0}^{\infty} \widetilde{g}_{qp}\phi_q(\theta)w_C(\theta)\rho_p(x), \quad (15)$$

with $w_C(\theta) = (1-\theta^2)^{-\frac{1}{2}}$ the orthogonal weight function of the Chebyshev polynomials, cf. [20] and $\widetilde{g}_{qp}$ the spectral coefficients of the weight function. Due to the orthogonality property of the Chebyshev and Fourier polynomials, implementing (14) and (15) in (13) reduces the feedback law to

$$u(t) = \sum_{p,q=0}^{\infty} \widetilde{v}_{qp}(t)k_{qp}, \quad (16)$$

where $k_{qp} = \frac{\pi H}{8}c_q c_p \widetilde{g}_{qp}$ and the factor $c_i = 2$ for $i = 0$ and $c_i = 1$ for $i > 0$, see [20].
Note that this feedback law enables control of individual Chebyshev-Fourier-cosine modes by appropriate choice of k_{qp}. This so-called modal control scheme thus enables efficient control of exactly the relevant lower order modes. Meaning that this feedback law practically is a full-state feedback, which significantly outperforms standard P-control for this boiling application [14].
The elements k_{qp} must be determined such that desired/satisfactory closed-loop dynamics are obtained. This can be done by putting the so-called closed-loop poles of the linearised system at desired/satisfactory locations. To determine these closed-loop poles, a characteristic equation is derived analogously to the derivation of (7). The closed-loop poles of the system are given by the $\mu \in \mathbb{C}$ that satisfy

$$\begin{aligned}\sum_{k=0}^{\infty} A_k\rho_k(x)\left[\sqrt{\alpha_k}\tanh(\sqrt{\alpha_k}H) + \tfrac{1}{\lambda}\gamma(x)\right] \\ + \sum_{k=0}^{\infty} A_k F_k\left[\tfrac{1}{\lambda}\gamma(x) - \sqrt{\alpha_0}\right] = 0,\end{aligned} \quad (17)$$

for all $x \in [0, L]$, for nontrivial A_k (i.e. $A_k \neq 0$ for at least one k). The parameter α_k is given by

$$\alpha_k = \left(\frac{k\pi}{L}\right)^2 + \frac{\mu}{\alpha}. \quad (18)$$

and the closed-loop contribution F_k equals

$$F_k = \frac{\sum_{q=0}^{\infty} k_{qk}\xi_q^k}{\lambda\sqrt{\alpha_0} - \sum_{q=0}^{\infty} k_{q0}\zeta_q} \frac{e^{-\sqrt{\alpha_0}H}}{\cosh(\sqrt{\alpha_k}H)} \quad (19)$$

Furthermore, $(A_0 \cdots A_\infty)$ is the spectrum of the eigenmode of the closed-loop system that corresponds to the computed pole μ. The coefficients ξ^k and ζ are the spectral coefficients of the Chebyshev expansion of $\cosh\left(\sqrt{\alpha_k}\frac{H}{2}(\theta+1)\right)$ and $e^{-\sqrt{\alpha_0}\frac{H}{2}(\theta+1)}$, respectively. Approximations to the poles of the closed-loop system can be found via discretisation of (17). Derivation of this expression and determination of the poles is discussed in full detail in [15].
Using this equation, the closed-loop poles for a specific feedback law, i.e. with the elements k_{nk} given, can be determined. By varying one of the elements of the feedback law, e.g. k_{00}, the poles will move away from their original position. By plotting the path the dominant poles describe as function of the controller element, a pole-trajectory plot can be obtained. Using these plots, controllers that result in satisfying closed-loop behaviour are designed.

3.2 Observer design

It is important to note that, in practical applications, the state $T(x, y, t)$ (and thus $v(x, y, t)$) can only be measured at a finite number of points on the fluid-heater interface. Therefore, the control law discussed in the above necessitates an observer or "state-estimator", see [14]. This observer estimates the temperature profile out of available measurements of the heater temperature at the measurement points.
We assume that measurements are available at $x = 0$ and $x = L$ on the fluid-heater interface, i.e. at the top left corner and the top right corner of the heater. The error between the measurements and the output of the observer is used to approximate the error $E(x, y, t)$ between system state $T(x, y, t)$ and observer state $Z(x, y, t)$, on the entire fluid-heater interface, i.e. for $y = H$, meaning $E_F^{\text{ap}} \approx E(x, H, t) = T(x, H, t) - Z(x, H, t)$. The approximation E_F^{ap} is given by the Fourier expansion of the error in the measurement points $\widetilde{x}_r = r/R$ for $r = 0, ..., R$ and $R = 1$,

$$E_F^{\text{ap}}(x) = \sum_{r,p=0}^{R} \frac{\eta_r}{2R} E_F(\widetilde{x}_r)\rho_r(\widetilde{x}_r)\eta_p\rho_r(x), \quad (20)$$

where $\eta_i = 1$ for $i = 0 \vee K$ and $\eta_i = 2$ for $0 < i < K$. As observer we employ a copy of the nonlinear system with injection of E_F^{ap} on the boundary segment where the measurements are available, i.e. at the fluid-heater interface.

The observer thus is governed by

$$\frac{\partial Z}{\partial t}(x, y, t) = \alpha\nabla^2 Z(x, y, t), \quad (21)$$

with the boundary conditions

$$\left.\frac{\partial Z}{\partial x}\right|_{x=0,L} = 0, \quad (22)$$

$$\left.\frac{\partial Z}{\partial y}\right|_{y=0} = -\frac{1}{\lambda}(Q_H + u(t)), \quad (23)$$

$$\left.\frac{\partial Z}{\partial y}\right|_{y=H} = -\frac{1}{\lambda}q_F(Z_F) + qE_F^{ap}(x), \quad (24)$$

where q is the observer gain by which the observer error dynamics must be stabilised. Local stability of the observer error dynamics can be guaranteed via analysis according to (17) of the linearised observer error dynamics.

3.3 Controller-observer combination

The stability of the closed-loop system is only guaranteed in a small region around the to-be-stabilised equilibrium (local asymptotic stability) as it is based on the linearisation of the nonlinear system and observer. The so-called region of attraction of the closed-loop system, i.e. the region in which initial states converge to the equilibrium, can not be determined, however. In the next section simulations are performed and it will be shown that in some cases this region of attraction can be quite large. For some heater heights it is not possible to stabilise the homogeneous transition boiling equilibrium and, although the observer state converges to the system state in those cases, the system state converges to a non-uniform (and therefore undesired) temperature profile.

4 Closed-loop Simulations

To determine the effectiveness of the control strategy discussed in the previous section, some simulations are done with the unstable transition towards film boiling is stabilised. It turns out that this transition state can only be stabilised for specific combinations of the heater properties λ (heater material) and L, H (heater dimensions), for given Q_H (nominal heat supply). This means that in the design of a thermal management system for EVs, it is important to determine the typical value for the heat generation Q_H and choose heater dimensions and material accordingly.
In the following, two case studies are discussed. The first represents the design of a cooling device for IGBTs and the second a thermal management and homogenisation scheme for a small battery cell. As the pressure can be varied only within a certain operating range, the input is restricted by $-0.8Q_H \leq u(t) \leq 2Q_H \; \forall \; t > 0$ in the simulations.

For the simulations, discretisation of the nonlinear system is accomplished by a Chebyshev-Fourier-cosine spectral method identical to that underlying (14) in combination with a second-order Cranck-Nicholson time-marching scheme [20]. This admits a highly accurate approximation of the underlying nonlinear PDE with reasonable finite resolutions. The discretised system is then solved for each Fourier-mode individually; their coupling via the boundary condition on $y = H$ is treated by a standard Picard iteration [19]. The initial conditions are constructed similarly as in [14]: $\widetilde{\mathbf{T}}(0) = \widetilde{\mathbf{T}}_\infty + \epsilon\mathbf{n}$, with $\widetilde{\mathbf{T}}_\infty$ the to-be-stabilised equilibrium and $\epsilon\mathbf{n}$ an exponentially-decaying Gaussian perturbation (standard deviation equals 1) with magnitude ϵ. In the following $\epsilon = 10^{-1}$ is taken.

4.1 IGBT-cooling

IGBTs are high-power switching devices used to switch large amounts of power from the battery pack to electrical coils, which produce about four times as much heat as a conventional computer chip. For this case study the heat generation Q_H is set to $Q_H = 15$ W/cm^2 see also [17]. For two different heater designs, i.e. the height of the heater is varied, the control strategy introduced above is applied to the system for stabilisation of the homogeneous transition state. It will be shown that the heater can not be made too thin as this promotes non-uniform temperature distributions in the device. The length of the heater in this case is $L = 80$mm, which is the length of an IGBT of dimensions 80×80mm.

4.1.1 Heater height: $H = 20$mm

The controller and observer parameters are taken according to

$$(k_{0,0}, k_{1,0}, k_{2,0}) = (-30, -10, 6.6), \quad q = 2, \tag{25}$$

and controller parameters for higher Fourier-Chebyshev modes, i.e. k_{nk} for $n > 3$ or $k > 0$, equal zero. In Fig.4 the simulated evolution of the interface temperature ($T_F(x,t) := T(x,H,t)$) is shown (progression in time is indicated by darker shades of grey of the intermediate profiles). This reveals a smooth progression from an essentially heterogeneous initial state, to the final homogeneous state. This means that disturbances that arise during operation can be suppressed effectively, resulting in constant and uniform temperatures. As can be seen the region of attraction is quite large in this case. Although the temperature of the IGBT is too high initially, the controller manages to remove the excess heat in the IGBT and the heater. As a result, the superheat drops to the desired value of 60K. Fig. 4 shows that the initial temperature fluctuations in x-direction are rapidly smoothed out, resulting in a homogeneous temperature distribution in the device.

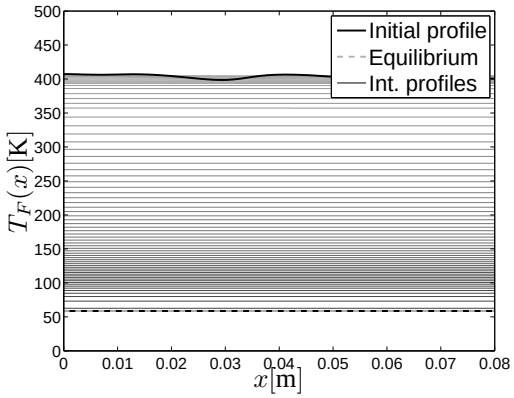

Figure 4: The evolution of the interface temperature $T_F(x,t)$ is shown for the IGBT-cooling case study, $H = 20$mm. The thin grey lines are intermediate profiles, progression in time is indicated by darker shades of grey.

The temperature as function of time in the points $(x,y) = (0,H)$, $(x,y) = (\frac{1}{2}L, H)$ and $(x,y) = (L,H)$, i.e. the validation points, of both system and observer is given in Fig. 5. It can be seen that the observer state quite rapidly converges to the system state, from whereon the system state converges to the equilibrium.

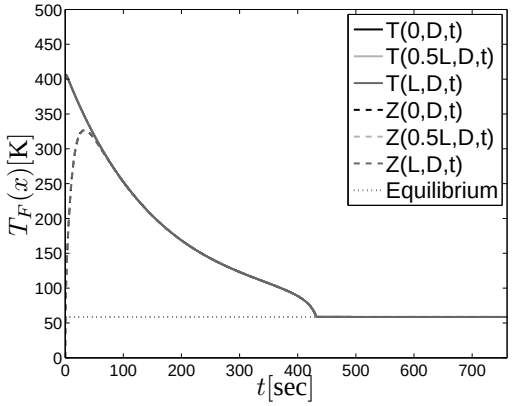

Figure 5: For the IGBT-cooling case study, $H = 20$mm, the evolution of the interface temperature of the system (solid line) and the observer (dashed line) are shown for $x = 0$, $x = \frac{1}{2}L$ and $x = L$.

Finally, the input used to stabilise the equilibrium is given as function of time in Fig. 6. Initially, the input is maximal due to the observers initial state, subsequently, the input is minimal until the temperature setpoint is reached.

4.1.2 Heater height: $H = 8$mm

If the heater is $H = 8$mm of height, the transition to film boiling can not be stabilised, since the interface temperature converges to a non-uniform

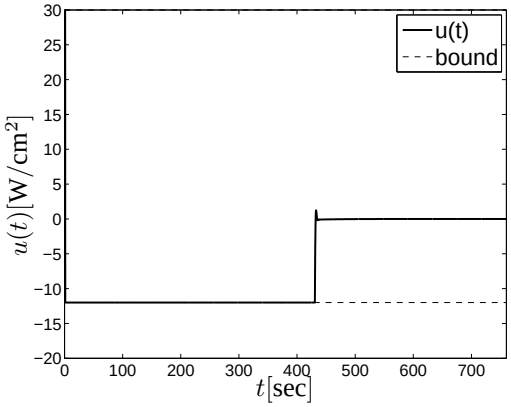

Figure 6: The input as function of time is shown for the IGBT-cooling case study, $H = 20$mm. The bounds of the input are given by the dashed lines.

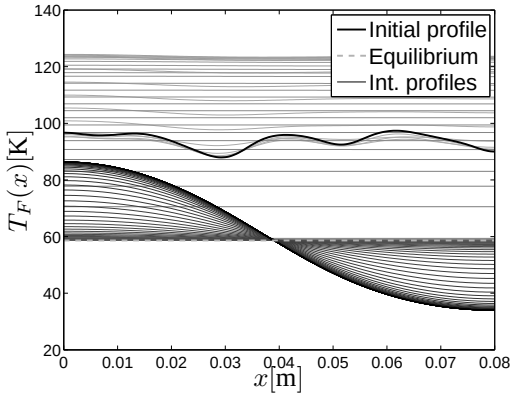

Figure 7: The evolution of the interface temperature $T_F(x,t)$ is shown for the IGBT-cooling case study, $H = 8$mm. The thin grey lines are intermediate profiles, progression in time is indicated by darker shades of grey.

state (partial vapour blanket). The controller and observer parameters are taken according to (25). The non-uniform state has temperatures that correspond to film boiling and regions with temperatures that correspond to nucleate boiling. The device thus will get very hot in some regions, while other regions still are well cooled. This phenomenon can not be avoided by taking different controller parameters as the homogeneous transition equilibrium is non-stabilisable for these system parameters. As the pressure can not be altered as function of x, the heat supply in our model must be varied uniformly. As a result, the system is not fully controllable. Depending on the system parameters the homogeneous transition equilibrium is then either stabilisable or non-stabilisable. In Fig. 7 the evolution of the fluid-heater interface temperature is shown. Although the initial condition is taken quite close the the equilibrium, the small perturbations are amplified by the boiling process resulting in the non-uniform temperature distribution. This results in a large temperature distribution in the device.

In Fig. 8 the evolution of the system and observer state in the validation points is given. Initially the observer state has a large deviation from the system state. As a result, the system state is regulated in opposite direction initially. After the observer state has converged on the system state, the system state is regulated towards the equilibrium. The non-uniformity thus is not the result of poor observer performance. After some time the system state starts to deviate from the equilibrium and convergence to a non-uniform state is observed.

In Fig. 9 the input as function of time is given. It can be seen that the input settles at a nonzero value after the system state has converged on the non-uniform state.

In some cases, the convergence on the non-uniform state can be remedied by varying the nominal pressure p (thus creating another equilibrium to stabilise). However, for these heater properties the only measure that can be taken, is a large safety margin between actual heat flux and

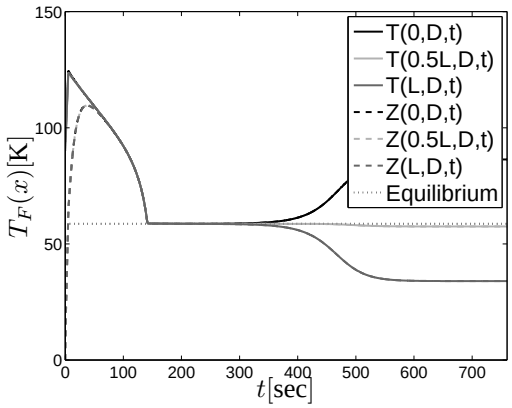

Figure 8: For the IGBT-cooling case study, $H = 8$mm, the evolution of the interface temperature of the system (solid line) and the observer (dashed line) are shown for $x = 0$, $x = \frac{1}{2}L$ and $x = L$.

critical heat flux (CHF). This will adversely affect the cooling efficiency, though.

4.2 Battery thermal management

The second case study is the thermal homogenisation of a small battery cell, like for example used in the Tesla Roadster. The same setup (Fig. 1) is used as thermal management scheme. Since the cells are closely packed together in a battery pack, the boiling chamber becomes very confined, thus significantly limiting the amount of boiling liquid. As a result, the net evaporation/condensation of the total amount of working fluid plays a significant role in the cooling process. Physical considerations suggest that in a first approximation this can be described by rescaling the boiling curve. The critical heat flux (CHF) will namely effectively decrease if

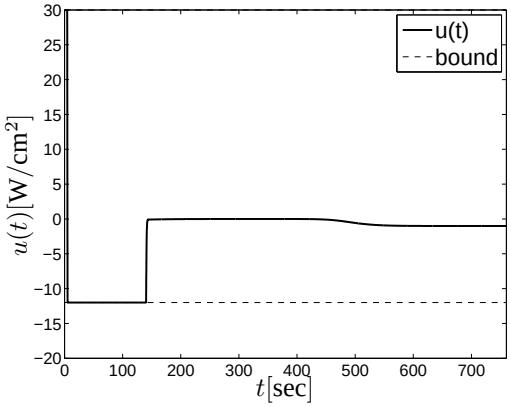

Figure 9: The input as function of time is shown for the IGBT-cooling case study, $H = 8$mm. The bounds of the input are given by the dashed lines.

the volume of the liquid phase of the boiling medium drops below a certain minimum due to net evaporation of the total amount of working fluid. For this case study the boiling curve given in Fig. 10 therefore is taken. The battery pack in the Tesla Roadster can deliver up to 200 kW of electric power at 95% efficiency, see [18]. This means the heat generation of an individual battery cell can be as high as approximately 0.33 W/cm^2. Hence, the heat generation is set to $Q_H = 0.33$W/cm^2 for this case study.

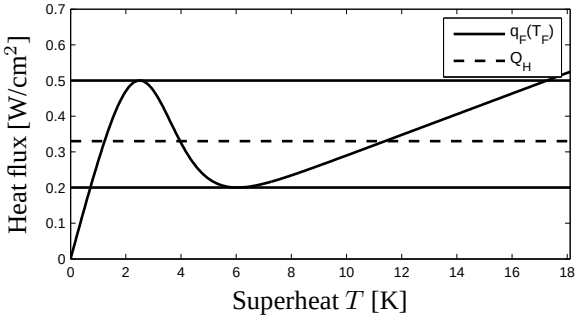

Figure 10: Nonlinear heat-flux function $q_F(T_F)$ according to the boiling curve of aluminum vs. FC-72, see [9]. The dashed line represents the nominal heat supply Q_H.

4.2.1 Heater height: $H = 3.5$mm

Controller and observer parameters are again according to (25). In Fig.11 the simulated evolution of the interface temperature ($T_F(x,t) := T(x,H,t)$) is shown (progression in time is again indicated by darker shades of grey of the intermediate profiles). Similar as for the IGBT cooling example an essentially heterogeneous initial state is regulated to the final homogeneous state. This means that disturbances that arise during operation can be suppressed effectively, resulting in constant and uniform temperatures in favour of a uniform temperature distribution throughout the battery pack. As can be seen, the region of attraction is quite large in this case as well. The too low initial temperature is increased by the controller by removing less heat from the battery. As a result, the battery warms itself until it reaches the desired temperature. The initial temperature fluctuations in x-direction are rapidly smoothed out, resulting in a homogeneous temperature distribution in the cell. This means temperature fluctuations can be smoothed very effectively by the thermal management scheme.

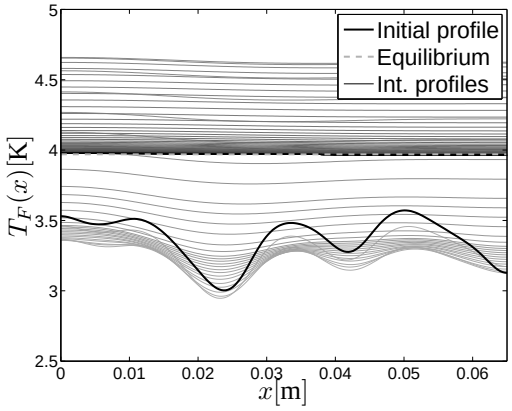

Figure 11: The evolution of the interface temperature $T_F(x,t)$ is shown for the battery-cooling case study, $H = 3.5$mm. The thin grey lines are intermediate profiles, progression in time is indicated by darker shades of grey.

The temperature as function of time in the validation points is given in Fig. 12. Again the observer state quite rapidly converges to the system state. Due to the initial error, the system overshoots its equilibrium value, however. After the observer state has reached the equilibrium the system state is regulated towards the equilibrium as well.
Finally, the input used to stabilise the equilibrium is given as function of time in Fig. 13. Initially, the input is taken maximal, then minimal and subsequently it smoothly converges to zero as the system state converges on the equilibrium.

4.2.2 Heater height: $H = 1.75$mm

If the heater is $H = 1.75$mm of height, the transition to film boiling can not be stabilised, since the interface temperature converges to a non-uniform state (partial vapour blanket). This represents a temperature non-uniformity in the battery cell, which is undesired. The controller parameters are taken according to (25). In Fig. 14 the evolution of the fluid-heater interface temperature is shown. Although the initial condition is taken quite close to the equilibrium, the small perturbations are amplified by the boiling process resulting in a non-uniform temperature distribution.

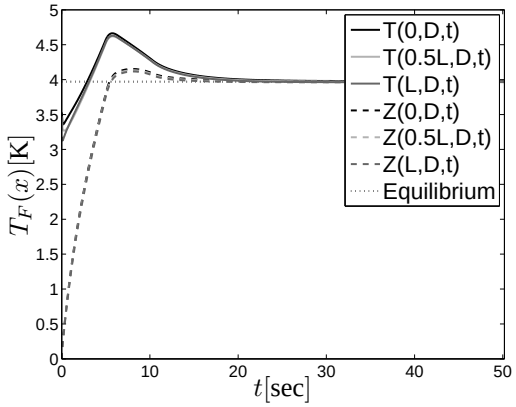

Figure 12: For the battery-cooling case study, $H = 3.5$mm, the evolution of the interface temperature of the system (solid line) and the observer (dashed line) are shown for $x = 0$, $x = \frac{1}{2}L$ and $x = L$.

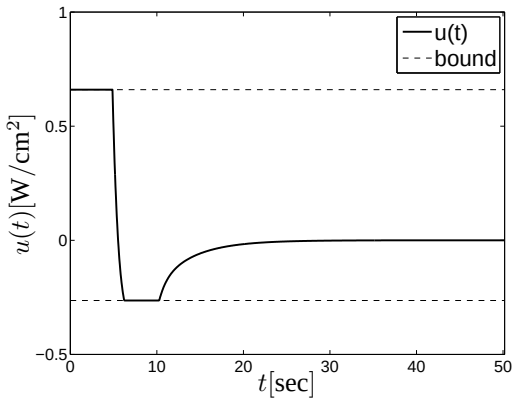

Figure 13: The input as function of time is shown for the battery-cooling case study, $H = 3.5$mm. The bounds of the input are given by the dashed lines.

As before, this can not be remedied by taking different controller parameters. Furthermore, the distributions represent local hot regions and local cold regions. Although the temperature non-uniformity does not exceed approximately 3K for this individual cell, it can accumulate to quite large differences in an entire battery pack.

Fig. 15 depicts the evolution of the system and observer state in the validation points. The figure shows that the non-uniformity is not the result of poor observer performance as the observer state converges to the system state quite rapidly. Furthermore, it can be seen that initially the controller keeps the system at its equilibrium, but then small fluctuations in x-direction are amplified and in the system converges to the non-uniform state.

In Fig. 16 the input as function of time is given. Again the input settles at a nonzero value due to the fact that the system has not converged on the equilibrium.

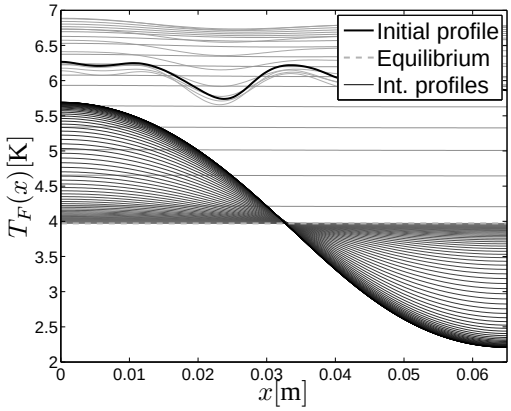

Figure 14: The evolution of the interface temperature $T_F(x,t)$ is shown for the battery-cooling case study, $H = 1.75$mm. The thin grey lines are intermediate profiles, progression in time is indicated by darker shades of grey.

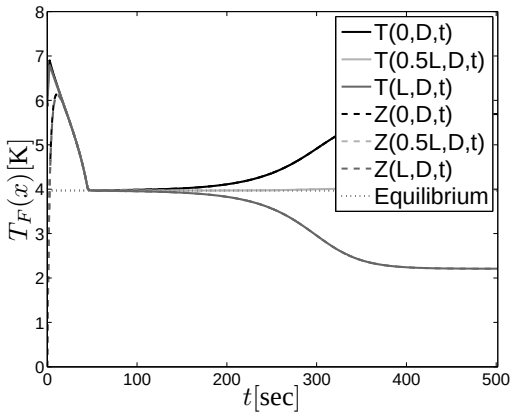

Figure 15: For the battery-cooling case study, $H = 1.75$mm, the evolution of the interface temperature of the system (solid line) and the observer (dashed line) are shown for $x = 0$, $x = \frac{1}{2}L$ and $x = L$.

5 Conclusion

In this study, a 2D nonlinear heat-transfer model for a boiling-based cooling device for cooling of Insulated Gate Bipolar Transistors (IGBTs) and battery thermal management in Electric Vehicles is considered. The model involves only the temperature distribution within the heater, i.e. a thermally conducting element between the to-be-cooled device and the boiling liquid. The heat exchange with the boiling medium is modelled via a nonlinear boundary condition imposed at the fluid-heater interface. In order to apply boiling at its fullest efficiency, unstable modes in the system must be stabilised.

To this end, a controller is introduced that regulates the pressure in the boiling system as a function of the heater temperature. by increasing (decreasing) the pressure, boiling can be sup-

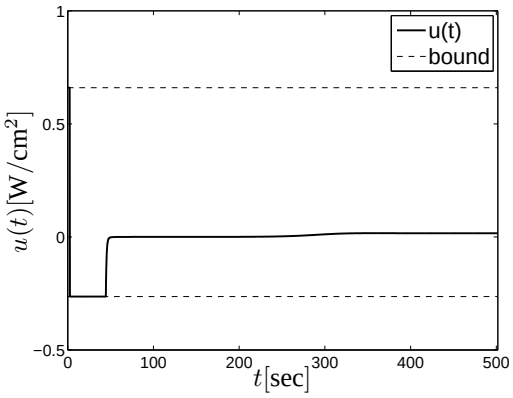

Figure 16: The input as function of time is shown for the battery-cooling case study, $H = 1.75$mm. The bounds of the input are given by the dashed lines.

pressed (stimulated) and as a result, more (less) heat can be extracted from the heater by the boiling liquid. In this way the boiling system can be kept in the efficient nucleate boiling regime. The entire temperature profile within the heater is estimated by an observer using only two measurements, both on top of the heater. Previous analyses have shown that controllers based on the dominant modes of the temperature profile within the heater are effective, see [16]. For this reason, the controller developed for this system is based on these modes as well.

The control strategy filters the Chebyshev-Fourier-cosine modes of the temperature profile of the heater. These modes are intimately related to the eigenmodes of the system. Therefore, the dynamics are mainly prescribed by the dominant modes, that is, the lower order Chebyshev-Fourier-cosine modes. The feedback law thus enables control of exactly those relevant lower order modes.

The observer is a copy of the nonlinear pool boiling model with an extra term in the boundary condition for the fluid heater interface, i.e. the top of the heater, by which convergence of the observer state on the system state is to be accomplished. This extra term accounts for the error between observer and system state on the fluid-heater interface.

Local asymptotic stability can be established via the linearised system and observer. Satisfactory closed-loop behaviour is obtained by fine-tuning of the control parameters using a characteristic equation which is derived using the method of separation of variables.

The performance of the control law for stabilisation of the nonlinear system is investigated in order to establish its value for practical purposes. Relevant issues are the asymptotic stability and evolution of the nonlinear closed-loop system. Simulations are performed for two case studies: (i) IGBT cooling and (ii) battery thermal management. It turns out that the closed-loop behaviour of the system is dependent on the system parameters such as height of the heater.

The first case study reveals convergence of the evolution of the nonlinear system on the unstable steady state for a wide range of initial states in case $H = 20$mm. These findings imply that the control loop indeed is capable of robustly stabilising the pool-boiling system for these parameters. For a thinner heater, $H = 8$mm, however, convergence of the nonlinear system on an essentially non-uniform state is observed. The final state has a region with temperatures corresponding to nucleate boiling ('cold spots') and has a region corresponding to film boiling ('hot spots'). This results in local 'hot-spots' on the IGBT and is highly undesired since it can lead to failure of the device. In some cases, this phenomenon can be remedied by varying the nominal pressure in the boiling chamber. However, for these heater properties the only measure is stabilisation of the nucleate boiling equilibrium. A safety margin needs to be taken into account for this measure, though, this affects the cooling efficiency negatively.

If boiling is applied to the individual cells in a battery pack, the net evaporation/condensation of the boiling liquid plays a significant role as the volume of the pool is much smaller due to the closely packed battery cells. Physical considerations suggest that this can in a first approximation be modelled by a rescaled boiling curve. Therefore, thermal management of these cells, in spite of their low heat generation, still is a challenge, since non-uniform temperatures and local 'hot spots' may still occur. The case study reveals that convergence to the unstable uniform transition boiling equilibrium can nonetheless be achieved for $H = 3.5$mm. For this case study, similar as for the IGBT-cooling case study, also convergence to a non-uniform state is observed for a thinner heater, i.e. $H = 1.75$mm. This is highly undesired in battery thermal management, as it leads to more rapid battery deterioration.

Nevertheless, both case studies show that the efficiency of boiling-based cooling schemes can be increased by dynamically varying the pressure inside the boiling chamber. This puts forth boiling heat transfer as a promising solution for thermal management issues in electric vehicles. During the design process heater material and dimensions must be chosen carefully, though.

Acknowledgements

This research is funded by the HTAS-REI (Range Extender Innovations) project.

References

[1] I. Besselink, J. Hereijgers, P. van Oorschot, and H. Nijmeijer, "Evaluation of 20000 km driven with a battery electric vehicle," in *Proc. EEVC*, (Brussels, Belgium), 2011.

[2] A. Pesaran, "Current and future needs in electric drive vehicle batteries," in *IHTC14*, (Washington DC), 2010.

[3] P. Ramadass *et al.*, "Capacity fade of sony 18650 cells cycled at elevated temperatures: Capacity fade analysis," *J. Power Sources*, vol. 112, pp. 614–620, 2002.

[4] A. Pesaran, A. Vlahinos, and S. Burch, "Thermal performance of EV and HEV battery modules and packs," in *Proc. 14th Int. EV Symp., Orlando*, 1997.

[5] R. van Gils, M. Speetjens, and H. Nijmeijer, "Boiling heat transfer in electric vehicles," Tech. Rep. DC 2011.52, Eindhoven U. of Tech., Dept. of Mech. Eng., 2011.

[6] H. van Ouwerkerk, "Burnout in pool boiling the stability of boiling mechanisms," *Int. J. Heat Mass Transfer*, vol. 15, no. 1, pp. 25–34, 1972.

[7] V. Dhir, "Boiling heat transfer," *Annu. Rev. Fluid Mech.*, vol. 30, pp. 365–401, 1998.

[8] I. Mudawar, "Assessment of high-heat-flux thermal management schemes," *IEEE Trans. Comp. Packaging Technol.*, vol. 24, no. 2, pp. 122–141, 2001.

[9] H. Auracher and W. Marquardt, "Heat transfer characteristics and mechanisms along entire boiling curves under steady-state and transient conditions," *Int. J. Heat Fluid Flow*, vol. 25, pp. 223–242, 2004.

[10] J. Blum, W. Marquardt, and H. Auracher, "Stability of boiling systems," *Int. J. Heat Mass Transfer*, vol. 39, no. 14, pp. 3021–3033, 1996.

[11] J. Blum *et al.*, "Temperature wave propagation as a route from nucleate to film boiling?," in *Proc. 2nd int. symp. two-ph. flow mod. and exp.*, (Rome, Italy), 1999.

[12] M. Speetjens, A. Reusken, and W. Marquardt, "Steady-state solutions in a nonlinear pool boiling model," *Com. Nonl. Sci. Num. Sim.*, vol. 13, pp. 1475–1494, 2008.

[13] M. Speetjens *et al.*, "Stability analysis of two-dimensional pool-boiling systems," *SIAM J. Applied Dyn. Sys.*, vol. 7, pp. 933–961, 2008.

[14] R. van Gils, M. Speetjens, and H. Nijmeijer, "Feedback stabilisation of a one-dimensional nonlinear pool-boiling system," *Int. J. Heat Mass Transfer*, vol. 53, pp. 2393–2403, May 2010.

[15] R. van Gils, M. Speetjens, and H. Nijmeijer, "Feedback stabilisation of a two-dimensional pool-boiling system by modal control," 2011. submitted for publication.

[16] R. van Gils, M. Speetjens, and H. Nijmeijer, "Feedback stabilisation of two-dimensional non-uniform pool-boiling states," in *Heat Transfer XI*, (Tallin, Estonia), pp. 215 – 226, WIT Press, 2010.

[17] R. Chu *et al.*, "Review of cooling technologies for computer products," *IEEE Trans. Device Materials Reliability*, vol. 4, pp. 568–585, 2004.

[18] G. Berdichevsky, K. Kelty, J. Straubel, and E. Toomre, "The tesla roadster battery system." Tesla Motors, August 16, 2006.

[19] E. Kreyszig, *Advanced Engineering Mathematics*. Wiley, New York, 1999.

[20] C. Canuto *et al.*, *Spectral Methods in Fluid Dynamics*. Springer, New York, 1987.

Authors

Rob van Gils received the M.Sc. degree (with great distinction) in Mechanical Engineering from Eindhoven University of Technology, in 2008. Since September 2008, he is a Ph.D. candidate with the Dynamics and Control group at the Mechanical Engineering Department of Eindhoven University of Technology.

Michel Speetjens received his PhD degree (with honours) in Applied Physics from Eindhoven University of Technology in 2001. During 2002-2005 he was postdoctoral researcher at CSIRO, Australia and RWTH-Aachen, Germany. Since 2006 he holds a position as assistant professor in thermal transport phenomena at Mechanical Engineering, Eindhoven University of Technology.

Henk Nijmeijer (1955) obtained his MSc-degree and PhD-degree in Mathematics from the University of Groningen, Groningen, the Netherlands, in 1979 and 1983, respectively. From 1983 untill 2000 he was affiliated with the Department of Applied Mathematics of the University of Twente, Enschede, the Netherlands. Since, 1997 he was also part-time affiliated with the Department of Mechanical Engineering of the Eindhoven University of Technology, Eindhoven, the Netherlands. Since 2000, he is a full professor at Eindhoven, and chairs the Dynamics and Control group.